available at www.sciencedirect.com

ScienceDirect

journal homepage: www.elsevier.com/locate/aca

Enhanced sensitivity for deoxyribonucleic acid electrochemical impedance sensor: Gold nanoparticle/polyaniline nanotube membranes

*Yuanyuan Feng, Tao Yang, Wei Zhang, Chen Jiang, Kui Jiao**

Key Laboratory of Eco-chemical Engineering (Ministry of Education of China), College of Chemistry and Molecular Engineering, Qingdao University of Science and Technology, Qingdao 266042, China

ARTICLE INFO

Article history:
Received 18 January 2008
Received in revised form
28 March 2008
Accepted 3 April 2008
Published on line 16 April 2008

Keywords:
Polyaniline nanotube
Gold nanoparticle
Deoxyribonucleic acid biosensor
Electrochemical impedance spectroscopy
Phosphinothricin acetyltransferase gene

ABSTRACT

Gold nanoparticle/polyaniline nanotube membranes on the glassy carbon electrode (Au/nanoPAN/GCE) were constructed for the electrochemical sensing of the immobilization and hybridization of DNA. The properties of the Au/nanoPAN/GCE, the characteristics of the immobilization and hybridization of DNA were studied by cyclic voltammetry, differential pulse voltammetry and electrochemical impedance spectroscopy. The synergistic effect of the two kinds of nanomaterials, nanogold and nanoPAN, could enhance dramatically the sensitivity for the DNA hybridization recognition. DNA sequence-specific of phosphinothricin acetyltransferase gene (PAT) existing in some transgenic crops was detected by electrochemical impedance spectroscopic measurement. The dynamic detection range of the sequence-specific DNA was from 1.0×10^{-12} to 1.0×10^{-6} mol L^{-1}, and the detection limit was 3.1×10^{-13} mol L^{-1}. This biosensor had much wider dynamic detection range and lower detection limit for the DNA detection as compared with other DNA biosensors reported by us. The biosensor also has good selectivity, stability and reproducibility.

© 2008 Elsevier B.V. All rights reserved.

1. Introduction

Polyaniline (PAN) has attracted a special attention [1] in the field of conducting macromolecule. On account of the homogeneity, unique redox properties, high electrical conductivity and strong adherence to electrode surface, PAN has been extensively applied in electrochemical biosensors [2–9]. Besides retaining electrochemical properties of traditional PAN, PAN nanomaterial owns many advantages, such as a large specific surface area and unique property to accelerate electron transfer. Therefore, the electrochemical biosensor based on PAN nanomaterial can greatly enhance the sensing sensitivity and selectivity [10,11]. Recently, Morrin et al. [12] fabricated an amperometric enzyme biosensor based on PAN nanoparticles. Zhou et al. [13] investigated a sensitive and selective amperometric glucose biosensor based on platinum microparticles dispersed in nano-fibrous PAN. Zhu et al. [14] presented a novel and sensitive electrochemical DNA biosensor based on electrochemically fabricated PAN nanowire and methylene blue (MB) for DNA hybridization detection. PAN hybrid materials, which combine PAN and other kinds of nanomaterials, especially metal nanoparticles [15], play an important role in some kinds of sensors, such as biosensors and electrochemical sensors [16–20]. Tian et al. [21] reported

* *Corresponding author*. Tel.: +86 532 84855977; fax: +86 532 84023927.
E-mail address: Kjiao@qust.edu.cn (K. Jiao).
0003-2670/$ – see front matter © 2008 Elsevier B.V. All rights reserved.
doi:10.1016/j.aca.2008.04.022

that PAN and mercaptosuccinic-acid-capped gold nanoparticles (MSAGNP) could form stable multilayer films prepared by the layer-by-layer method. The films could electrocatalyze the oxidation of β-nicotinamide adenine dinucleotide (NADH) and could be utilized to detect DNA hybridization either by an electrochemical method or by surface plasmon enhanced fluorescence spectroscopy (SPFS). Both methods could effectively discriminate complementary DNA from noncomplementary DNA, even at the single-base mismatch level.

In this study, a DNA electrochemical biosensor based on gold nanoparticles/polyaniline nanotube membranes (Au/nanoPAN) formed in the presence of chitosan was prepared. The sensing composite membranes combined the very large surface areas of two kinds of nanomaterials with their excellent conductivities, and the attractive biocompatibility of gold nanoparticles to DNA molecules with the fine film-forming ability of chitosan. The synergistic effect of the nanoparticles could dramatically enhance the DNA attachment quantity and the detection sensitivity of DNA sequence. Cyclic voltammetry (CV) and electrochemical impedance spectroscopy (EIS) were used to the characterization of the composite films. EIS was also used for studying the immobilization and hybridization of probe DNA. This DNA electrochemical biosensor was used to detect the sequence-specific DNA of the PAT gene with the linear range from 1.0×10^{-12} to 1.0×10^{-6} mol L^{-1} and the detection limit of 3.1×10^{-13} mol L^{-1}.

2. Experimental

2.1. Materials

$HAuCl_4 \cdot 4H_2O$ and tris (hydroxymethyl) amminomethane (Tris) were purchased from Sigma (St. Louis, MO, USA). The diameter of nanoPAN is about 100 nm with a thickness of 30–50 nm [22], which was provided by College of Material Science and Engineering, Qingdao University of Science and Technology and used without further purification. The scanning electron microscopy (SEM) image of nanoPAN was shown in Fig. 1. Sodium dodecylsulfate (SDS) was purchased from Shanghai Reagent Company (Shanghai, China) and used as received. Potassium ferricyanide ($K_3[Fe(CN)_6]$) and potassium ferrocyanide ($K_4[Fe(CN)_6]$) were purchased from Shanghai No.1 Reagent Factory (Shanghai, China) and Shanghai Heng Da Chemical Co. Ltd. (Shanghai, China), respectively. All the chemicals are of analytical grade and solutions were prepared with ultrapure water.

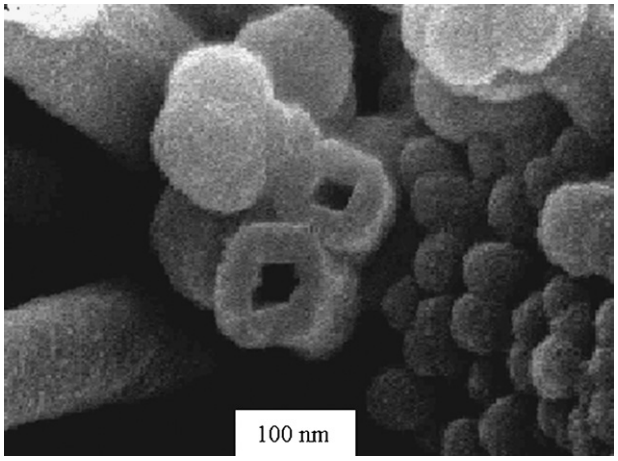

Fig. 1 – SEM image of polyaniline nanotube.

The 20-base oligonucleotides probe (ssDNA), its complementary sequence DNA (cDNA, target DNA, namely a 20-base fragment of PAT gene sequence, which was selected according to the transgenic sequence of phosphinothricin acetyltransferase gene), single-base mismatched DNA, double-base mismatched DNA and noncomplementary sequence DNA (ncDNA) were synthesized by Beijing SBS Gene Technology Limited Company (Beijing, China). Their base sequences are as below:

DNA probe (ssDNA): 5′-NH_2-GCC ACA AAC ACC ACA AGA GT-3′;
target DNA: 5′-ACT CTT GTG GTG TTT GTG GC-3′;
single-base mismatched DNA: 5′-ACT CTG GTG GTG TTT GTG GC-3′;
double-base mismatched DNA: 5′-ACT CTG GTG GTG CTT GTG GC-3′;
ncDNA: 5′-CAT GGT TGA TCC GTT CGC TG-3′.

All oligonucleotides stock solutions of 20-base oligomers (1.0×10^{-5} mol L^{-1}) were prepared using Tris–HCl solution (5.0 mmol L^{-1} Tris–HCl, 50.0 mmol L^{-1} NaCl, pH 7.0), which were stored at 4 °C. More diluted solutions were obtained via diluting aliquot of the stock solution with ultrapure water prior to use. The hybridization solution (pH 7.0) was diluted with 2 × SSC, which consisted of 0.30 mol L^{-1} NaCl and 0.03 mol L^{-1} sodium citrate tribasic dihydrate ($C_6H_5Na_3O_7 \cdot 2H_2O$).

2.2. Instrumentation

A CHI 660B electrochemical analyzer (Shanghai CH Instrument Company, Shanghai, China), which was in connection with a glassy carbon modified working electrode (Φ = 2 mm), a saturated calomel reference electrode (SCE) and a platinum wire auxiliary electrode, was used for the electrochemical measurement. The pH values of all solutions were measured by a model pHS-25 digital acidometer (Shanghai Leici Factory, Shanghai, China). Scanning electron microscopy was carried out using a JSM-5900 machine (JEOL, Tokyo, Japan). All solutions were prepared with Aquapro ultrapure water (Ever Young Enterprises Development. Co., Ltd., Chongqing, China).

2.3. Procedures

2.3.1. Preparation of the Au/nanoPAN/GCE

The glassy carbon electrode (GCE) surface was freshly polished prior to each experiment with 1, 0.3, and 0.05 μm α-Al_2O_3 paste, respectively, and rinsed with ultrapure water after each polishing step, then cleaned ultrasonically in water and 95% ethanol, respectively, for 3 min each.

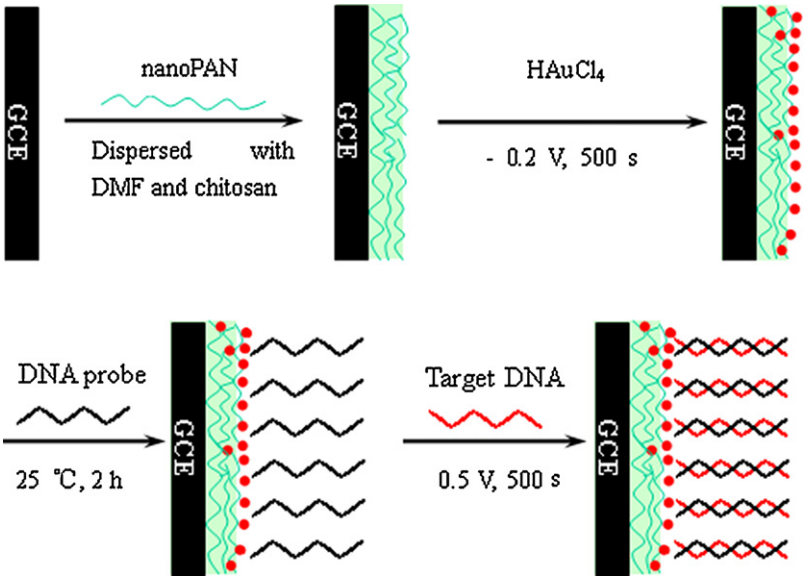

Fig. 2 – Schematic diagram of the immobilization and hybridization of DNA on Au/nanoPAN/GCE.

1.0 g L^{-1} nanoPAN dispersed in *N*,*N*-dimethylformamide (DMF) was mixed with chitosan solution (sonicated for 1 h), in a volume ratio of 1:50. 6 μL of above solution was coated onto the fresh surface of the GCE and air-dried naturally to obtain nanoPAN/GCE.

The nanoPAN/GCE was immersed into a 3.0 mmol L^{-1} $HAuCl_4$ solution containing 0.1 mol L^{-1} KNO_3, electrodepositing for 500 s at −200 mV. The obtained electrode was denoted as Au/nanoPAN/GCE.

2.3.2. *DNA probe immobilization and hybridization*

Immobilization of DNA probes was performed by immersing the Au/nanoPAN/GCE into 2.0 mL Tris–HCl buffer (pH 7.0) solution containing 1.0×10^{-6} mol L^{-1} DNA probe for 2 h at room temperature, followed by washing the electrode with 0.2% SDS solution and ultrapure water, respectively, for 5 min each to remove the unbound DNA probes.

The probe DNA/Au/nanoPAN/GCE was immersed in a hybridization solution (2 × SSC buffer, pH 7.0) containing the target DNA and hybridized for 500 s at +0.5 V, followed by washing the electrode with 0.2% SDS to remove the unhybridized DNA. The schematic representations of the immobilization and hybridization of DNA on the Au/nanoPAN/GCE were shown in Fig. 2.

2.3.3. *Electrochemical measurements*

The CV and EIS measurements were performed with a CHI 660B Electrochemical Analyzer. CV was recorded between 0.6 and −0.3 V at a scan rate of 100 mV s^{-1} in 1.0 mmol L^{-1} $K_3[Fe(CN)_6]$ and 1.0 mmol L^{-1} $K_4[Fe(CN)_6]$ (1:1) solution containing 0.1 mol L^{-1} KCl.

The AC voltage amplitude was 5 mV and the voltage frequencies range from 10^5 to 0.05 Hz in the EIS measurements. The applied potential was 172 mV vs. SCE. The above solution was also used as the supporting electrolyte solution for the EIS experiments.

3. Results and discussion

3.1. *Electrochemical characteristics of the Au/nanoPAN/GCE*

3.1.1. *Cyclic voltammetric behavior of the Au/nanoPAN/GCE*

CVs at the bare GCE and the different modified electrodes in 1.0 mmol L^{-1} $[Fe(CN)_6]^{3-/4-}$ were shown in Fig. 3. A couple of well-defined redox peaks could be observed at the bare GCE (curve a) with the cathodic peak current (i_{pc}) of 2.429×10^{-5} A and the anodic peak current (i_{pa}) of -2.428×10^{-5} A. The peak currents at the Au/GCE (curve b) increased dramatically in comparison with those of curve a. The reason was that nanoAu with large specific surface area and good conductivity could act as tiny conduction centers which facilitate the transfer of

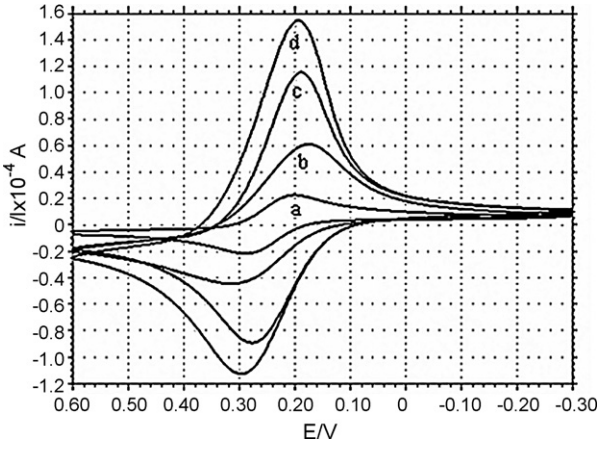

Fig. 3 – Cyclic voltammograms of 1.0 mmol L^{-1} $K_4[Fe(CN)_6]/K_3[Fe(CN)_6]$ (1:1) in 0.1 mol L^{-1} KCl recorded at (a) bare GCE, (b) Au/GCE, (c) nanoPAN/GCE and (d) Au/nanoPAN/GCE. Scan rate: 100 mV s^{-1}.

electrons, so it could accumulate much more $[Fe(CN)_6]^{3-/4-}$ on the modified electrode. The curve c (nanoPAN/GCE) showed a couple of redox peaks with high peak currents, indicating that the nanoPAN modified electrode had a much larger effective surface area and also good electrical conductivity [10]. In particular, the cooperation of nanoPAN and nanoAu in the modified film amplified the peak current greatly. Compared with curves b and c, CV at the Au/nanoPAN/GCE (curve d) had a couple of well-defined redox peaks with further enhanced peak currents (i_{pc} 1.478×10^{-4} A and i_{pa} -1.041×10^{-4} A). Herein, the synergistic amplification effect of the nanoPAN and nanoAu on enhancing the peak currents was outstanding.

3.1.2. *Electrochemical impedance spectroscopy of the Au/nanoPAN/GCE*

It is well known that EIS is a useful method for studying the surface properties of the modified electrode. In the Nyquist diagram, the semicircle diameter of the electrochemical impedance spectroscopy equals to the surface electron transfer resistance (R_{et}). The EISs at the bare GCE and the different modified electrodes in 1.0 mmol L^{-1} $[Fe(CN)_6]^{3-/4-}$ were shown in Fig. 4. Significant difference of R_{et}s was observed upon the stepwise formation of the modified electrode. The R_{et} value for the bare GCE (curve a) was 3.046×10^3 Ω. After the nanoAu film was assembled on the GCE, the R_{et} value was found to be 1.413×10^3 Ω (curve b). As compared with curve a, the R_{et} value of curve b reduced obviously. This might be due to the presence of nanoAu, which played an important role in accelerating the transfer of the electrons. After the bare GCE was modified with nanoPAN, the R_{et} value (7.491×10^2 Ω) decreased obviously (curve c), implying that nanoPAN was more facile to the electron transfer. For the Au/nanoPAN/GCE, the R_{et} value (2.398×10^2 Ω) decreased further (curve d). The result is consistent with that in Fig. 3.

3.1.3. *Selection of the ratio of nanoPAN to chitosan for preparing nanoPAN/GCE*

The ratio of nanoPAN to chitosan had a pronounced effect on the performance of the composite film modified electrode. Different volume ratios of nanoPAN to chitosan, such as 1:90, 1:70, 1:50, 1:30 and 1:10, were tested. The performance of the nanoPAN/GCE was characterized by differential pulse voltammetry (DPV). The correspondence of the volume ratio of nanoPAN to chitosan ($V_{nanoPAN}$:V_{CHIT}) on the DPV reductive peak current difference (ΔI_P) of $[Fe(CN)_6]^{3-/4-}$ between nanoPAN/GCE and bare GCE was shown in Fig. 5. The histogram showed that the ΔI_P increased with the increase of $V_{nanoPAN}$:V_{CHIT} and reached a maximum value at $V_{nanoPAN}$:V_{CHIT} of 1:50. Then, the ΔI_P decreased with the further increase of the nanoPAN content. Probably too great amount of nanoPAN could be coagulated and led to the lower conductivity [23,24]. The optimal ratio of $V_{nanoPAN}$:V_{CHIT} was 1:50.

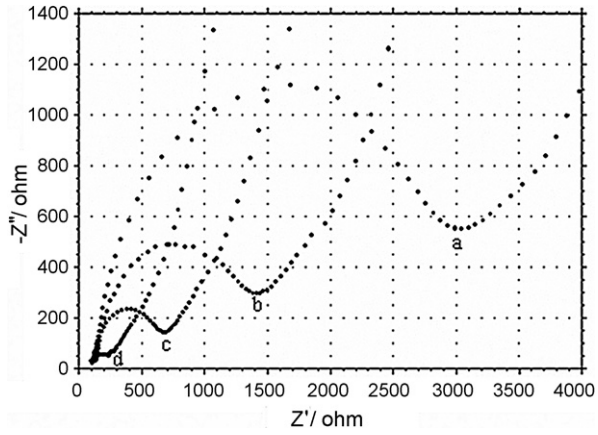

Fig. 4 – Nyquist diagrams recorded at (a) bare GCE, (b) Au/GCE, (c) nanoPAN/GCE and (d) Au/nanoPAN/GCE. Supporting electrolyte solution is 1.0 mmol L^{-1} $K_4[Fe(CN)_6]/K_3[Fe(CN)_6]$ (1:1) containing 0.1 mol L^{-1} KCl.

3.1.4. *Optimum of nanoAu immobilization*

The immobilization of nanoAu on the nanoPAN/GCE was carried out using two different methods: the constant potential deposition in $HAuCl_4$ solution [25] and dropping Au colloids

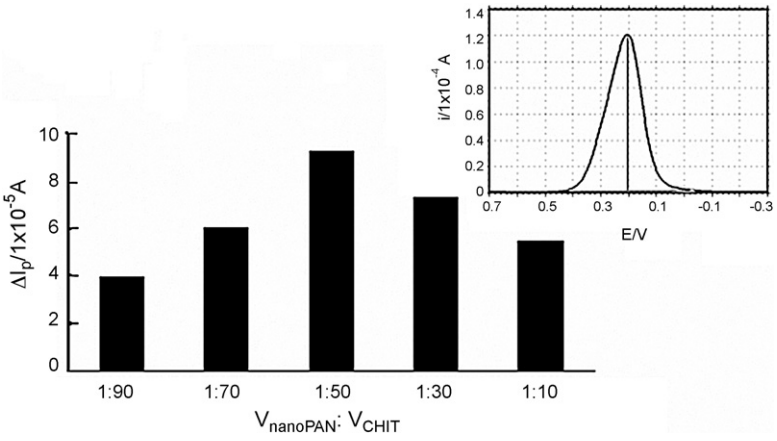

Fig. 5 – Effect of the ratio of $V_{nanoPAN}$:V_{CHIT} in composite on DPV reductive peak current difference (ΔI_P) of 1.0 mmol L^{-1} $K_4[Fe(CN)_6]/K_3[Fe(CN)_6]$ (1:1) between nanoPAN/GCE and bare GCE. The inset shows differential pulse voltammogram recorded at nanoPAN/GCE ($V_{nanoPAN}$:V_{CHIT} = 1:50). Supporting electrolyte solution is 1.0 mmol L^{-1} $K_4[Fe(CN)_6]/K_3[Fe(CN)_6]$ (1:1) containing 0.1 mol L^{-1} KCl. DPV parameters: pulse amplitude, 50 mV; pulse period, 0.2 s; pulse width, 60 ms.

[21,26] on the nanoPAN/GCE directly. The immobilization of nanoAu was evaluated according to the DPV reductive peak current difference (ΔI_P) of 1.0 mmol L^{-1} $[Fe(CN)_6]^{3-/4-}$ solution containing 0.1 mol L^{-1} KCl between Au/nanoPAN/GCE and nanoPAN/GCE. The results showed that the constant potential deposition in $HAuCl_4$ solution could immobilize much larger amount of nanoAu and obtain a bigger ΔI_P. This approach was used in the following experiments.

The concentration of $HAuCl_4$, the depositing potential and depositing time of nanoAu had pronounced effect on the performance of nanoAu modified electrode. If the concentration of $HAuCl_4$ was lower than 1.0 mmol L^{-1}, the growth rate of gold nanoparticles was too slow. If the concentration of $HAuCl_4$ was higher than 3.0 mmol L^{-1}, the nucleation and growth rate of gold nanoparticles were too rapid, which could form aggregates of gold nanoparticles on the electrode surface. 3.0 mmol L^{-1} $HAuCl_4$ solution was optimal for the loading of nanoAu [25]. If the depositing potential was more positive than −200 mV, the size and growth rate of gold nanoparticles were small, leading to an obvious decrease in ΔI_P response. If the depositing potential was more negative than −200 mV, the nucleation and the growth rate of gold nanoparticles were high, also leading to a decrease of the ΔI_P response. −200 mV of depositing potential was selected in experiments. The ΔI_P value increased gradually with the increase of electrodepositing time of nanoAu and reached a maximum when the depositing time was 500 s. After that, the ΔI_P value decreased slightly. Therefore, 500 s of electrodepositing time was selected.

3.2. *Impedance-based studies on DNA immobilization and hybridization*

3.2.1. *Electrochemical impedance spectroscopy of DNA immobilization and hybridization*

Fig. 6 shows the Nyquist diagrams of 1.0 mmol L^{-1} $[Fe(CN)_6]^{3-/4-}$ at the probe DNA/Au/nanoPAN/GCE (a), the hybridized dsDNA/Au/nanoPAN/GCE (b), the probe DNA/Au/GCE (c) and the hybridized dsDNA/Au/GCE (d). R_{et} value of curve a is 7.963×10^2 Ω, which is much larger than that of curve c (Au/nanoPAN/GCE) in Fig. 4. The change of the R_{et} value after modification was strong proof that the DNA probe had been immobilized on the Au/nanoPAN/GCE surface. The negatively charged phosphate backbone of the DNA probe prevented $[Fe(CN)_6]^{3-/4-}$ from reaching the electrode surface, leading to a much larger R_{et} value. After hybridization of the DNA probe with the target DNA, the R_{et} value increased greatly (curve b) to 2.778×10^3 Ω. The difference of the R_{et} values (ΔR_{et}) between at the hybrid electrode and at the probe electrode can be used for the evaluation of hybridization. Obviously, the impedance measurements further confirmed that the probe DNA/Au/nanoPAN/GCE could successfully recognize and detect the target DNA.

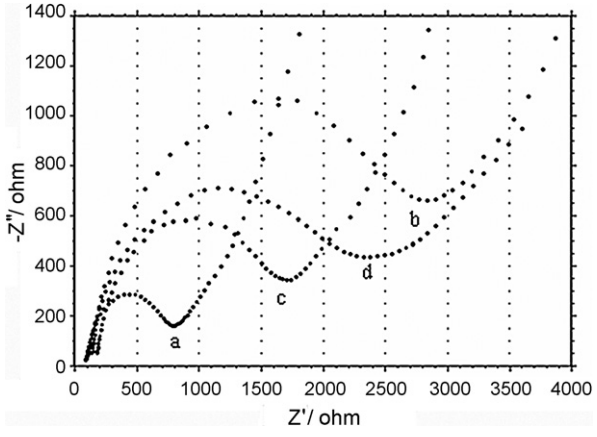

Fig. 6 – Nyquist diagrams recorded at (a) probe DNA/Au/nanoPAN/GCE, (b) dsDNA/Au/nanoPAN/GCE, (c) probe DNA/Au/GCE and (d) dsDNA/Au/GCE. Supporting electrolyte solution is 1.0 mmol L^{-1} $K_4[Fe(CN)_6]/K_3[Fe(CN)_6]$ (1:1) containing 0.1 mol L^{-1} KCl.

From curve c and curve d, the probe DNA/Au/GCE could also recognize and detect the target DNA. However, the ΔR_{et} value at the probe DNA/nanoPAN/Au/GCE is much larger than that at the probe DNA/Au/GCE, which demonstrated that nanoPAN has played an important role in the immobilization and hybridization of DNA.

The following experiment can further clarify the important role of nanoPAN. From the method of the previous literatures [27,28], the surface densities of the probe DNA on the nanoPAN/Au/GCE and on the Au/GCE were evaluated. The brief principle of this method is firstly to calculate the mol quantity of MB from the cyclic voltammetry, based on following equation: $N = Q/(neNA)$, where N represents the mol quantity of MB; Q the electric charge quantity of MB reduction process; n the number of electrons participating in the reaction, $n = 2$ in this experiment; e the electric charge quantity of one electron, which is 1.6×10^{-19} C; NA Avogadro's number, 6.02×10^{23} mol^{-1}. From our experiment, Q is 1.56×10^{-5} C and so N is 8.11×10^{-11} mol for the probe DNA/nanoPAN/Au/GCE, and Q is 1.08×10^{-5} C and N is 5.61×10^{-11} mol for the probe DNA/Au/GCE. Then, the surface density of the DNA probe can be calculated because one MB molecule can be combined with one G base. One DNA probe sequence, which contains three G bases, can combine three MB molecules in our experiment. The surface density of the DNA probe on the Au/nanoPAN/GCE was estimated to be 8.60×10^{-10} mol cm^{-2} and that on the Au/GCE to be 5.95×10^{-10} mol cm^{-2}. The results clarified that nanoPAN can enhance the loading of the DNA probe on the modified electrode.

3.2.2. *Immobilization conditions of DNA probe*

The immobilization of the DNA probe on the Au/nanoPAN/GCE was tested by three different methods, namely, by immersing adsorption, by dropping the DNA probe solution on the surface of the Au/nanoPAN/GCE and by electrodepositing the DNA probe on the surface of the Au/nanoPAN/GCE at a constant potential. The first method was that the Au/nanoPAN/GCE was immersed into a 2 mL 1.0×10^{-6} mol L^{-1} DNA probe of Tris–HCl buffer solution (pH 7.0) for different times at room temperature, such as 20 min, 40 min, 1 h and 2 h. The second method was carried out by dropping 10 μL above DNA probe solution on the surface of the Au/nanoPAN/GCE, followed by drying it at room temperature. The third method was carried out as follows: the Au/nanoPAN/GCE was immersed into a 2 mL above DNA probe solution and then electrochemical deposition was conducted at different potentials for different times. After

immobilization of the DNA probe the electrode was washed with 0.2% SDS solution and ultrapure water for 5 min, respectively. Then the Nyquist diagrams in $[Fe(CN)_6]^{3-/4-}$ solution at the Au/nanoPAN/GCE and the probe DNA/Au/nanoPAN/GCE were respectively recorded. The difference of the R_{et} values (ΔR_{et}) between at the probe DNA/Au/nanoPAN/GCE and at the Au/nanoPAN/GCE was evaluated. The largest ΔR_{et} value was obtained with the immersing adsorption for 2 h at room temperature. So we used immersing adsorption method to immobilize DNA probe in our experiments.

3.2.3. *Optimization of hybridization potential and time*

The hybridization potential and hybridization time were optimized via EIS experiments. The probe DNA/Au/nanoPAN/GCE was hybridized by immersing it into a stirring hybridization solution containing 1.0×10^{-6} mol L^{-1} target DNA at different potentials, such as 0.3, 0.4, 0.5, 0.6 and 0.7 V, for different times (200–700 s). The Nyquist diagrams of 1.0 mmol L^{-1} $[Fe(CN)_6]^{3-/4-}$ solution containing 0.1 mol L^{-1} KCl at the probe DNA/Au/nanoPAN/GCE and at the hybrid DNA/Au/nanoPAN/GCE were respectively recorded. The ΔR_{et} value was evaluated. The larger the ΔR_{et} value was, the better the hybridization. The largest ΔR_{et} value was obtained when the hybridization was conducted at 0.5 V for 500 s. Thus, the optimal hybridization potential was selected as 0.5 V and the optimal hybridization time as 500 s.

3.3. *Electrochemical detection of sequence-specific DNA of PAT gene*

3.3.1. *Selectivity of DNA hybridization recognition*

The ΔR_{et} value was used to be the measurement signal to determine the sequence-specific DNA of PAT gene.

The selectivity of this assay was investigated by using the DNA probe to hybridize with different DNA sequences. After hybridization of the DNA probe, the changes of the Nyquist diagram of $[Fe(CN)_6]^{3-/4-}$ were shown in Fig. 7. The curve a was the Nyquist diagram at the probe DNA/Au/nanoPAN/GCE. After hybridization of the DNA probe with the complementary DNA under the optimal experimental conditions, the change of the Nyquist diagram was shown as in curve b. The R_{et} value increased obviously, suggesting that hybrids (dsDNA) were formed at the electrode. The increase of the R_{et} value was negligible after the DNA probe was hybridized with the noncomplementary sequence (curve e), indicating that the hybridization reaction was not achieved. After the DNA probe was hybridized with single-base mismatched sequence (curve c) or double-base mismatched sequence (curve d), the increase of the R_{et} value was much smaller than that obtained from the hybridization with the complementary DNA sequence (curve b). And the single-base mismatched sequence and the double-base mismatched sequence could also be recognized via comparing the increase of the R_{et} value. The results demonstrated that this DNA biosensor displayed very high selectivity for the DNA hybridization detection.

3.3.2. *Sensitivity of DNA hybridization recognition*

Fig. 8 shows the Nyquist diagrams at the probe DNA/Au/nanoPAN/GCE electrode and the dsDNA/Au/nanoPAN/GCE

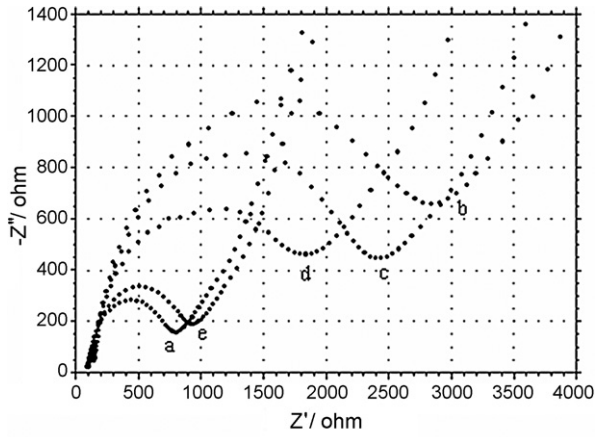

Fig. 7 – Nyquist diagrams recorded at (a) probe DNA/Au/nanoPAN/GCE, (b) dsDNA/Au/nanoPAN/GCE (hybridization with cDNA), (c) the electrode hybridized with single-base mismatched DNA, (d) the electrode hybridized with double-base mismatched DNA and (e) the electrode hybridized with ncDNA. Supporting electrolyte solution is 1.0 mmol L^{-1} $K_4[Fe(CN)_6]/K_3[Fe(CN)_6]$ (1:1) containing 0.1 mol L^{-1} KCl.

electrodes hybridized with different concentrations of sequence-specific DNA of PAT gene, ranging from 1.0×10^{-12} to 1.0×10^{-6} mol L^{-1}.

The ΔR_{et} value between before and after hybridization was linear with the logarithm of the sequence-specific DNA concentrations. The dynamic detection range for the sequence-specific DNA of PAT gene was from 1.0×10^{-12} to 1.0×10^{-6} mol L^{-1} with the regression equation ΔR_{et} (Ω) = 3.072 lg C + 36.539 and the regression coefficient (γ) 0.9959. The detection limit was 3.1×10^{-13} mol L^{-1} using 3σ, where σ was the standard deviation of 11 parallel measurements of the blank solution. The result demonstrated that the sensitivity of

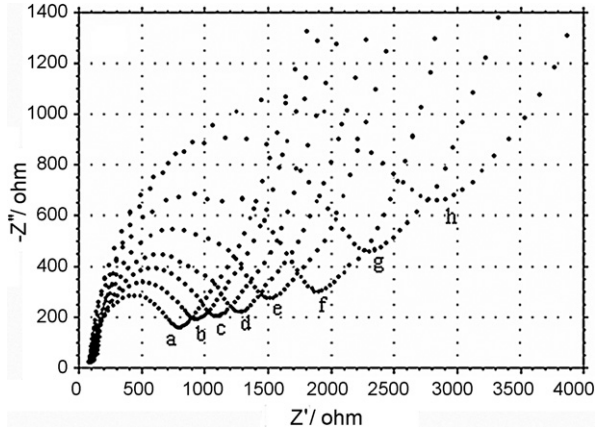

Fig. 8 – Nyquist diagrams recorded at the probe DNA/Au/nanoPAN/GCE (a) and after hybridization reaction with different concentrations of sequence-specific DNA of PAT gene: (b) 1.0×10^{-12} mol L^{-1}, (c) 1.0×10^{-11} mol L^{-1}, (d) 1.0×10^{-10} mol L^{-1}, (e) 1.0×10^{-9} mol L^{-1}, (f) 1.0×10^{-8} mol L^{-1}, (g) 1.0×10^{-7} mol L^{-1} and (h) 1.0×10^{-6} mol L^{-1}.

Table 1 – Comparison of the proposed biosensor with others for DNA specific sequence detection of PAT gene

Method	This work	Ref. [25]	Ref. [28]
Films for DNA immobilization	Au/nanoPAN/GCE	Au/PDC/GCE	$NanoZrO_2$/SWNTs/PDC/GCE
Detection limit (mol L^{-1})	3.1×10^{-13}	2.4×10^{-11}	1.38×10^{-12}
Detection range of target DNA (mol L^{-1})	1.0×10^{-12} to 1.0×10^{-6}	1.0×10^{-10} to 1.0×10^{-5}	1.0×10^{-11} to 1.0×10^{-6}

this impedance-based DNA sensor was good enough for the PAT gene sequence detection. At the same time, the detection range was very wide.

The proposed biosensor was compared with other DNA electrochemical biosensors reported in literatures for DNA specific sequence detection of the PAT gene, as listed in Table 1. This DNA biosensor had a lower detection limit and wider dynamic detection range for the target DNA assay than the other two.

3.3.3. *Reproducibility and regeneration of the DNA biosensor*

Six parallel-made DNA sensors were used to detect 1.0×10^{-10} mol L^{-1} target DNA, and the response ΔR_{et} values were respectively 4.827, 4.906, 4.869, 4.845, 4.794 and 4.813 ($\times 10^2\ \Omega$) with a relative standard deviation of 4.05% ($n = 6$). The results indicated that the reproducibility of this DNA biosensor was satisfactory.

The regeneration ability of this impedance-based DNA hybridization sensor was also evaluated by denaturing the hybridized dsDNA on the electrode surface, and the regenerated probe DNA/Au/nanoPAN/GCE was used repetitively. The hybridized dsDNA was hot denatured by immersing the electrode into boiling water for 10 min, and then it was cooled down rapidly with an ice salt bath, followed by rinsing the electrode with the ultrapure water. The Nyquist diagrams of 1.0 mmol L^{-1} $[Fe(CN)_6]^{3-/4-}$ solution at the regenerated probe DNA/Au/nanoPAN/GCE and the hybridized dsDNA/Au/nanoPAN/GCE were recorded. The results indicated that the two R_{et} values and ΔR_{et} value were almost the same values as those obtained in the first experiment. Repetitive experiments showed that the DNA sensor could be reproduced for three times without losing its sensitivity. In addition, the sensor was stable for at least 10 days upon storage at 4 °C in a dry state, indicating the fine regeneration ability of the biosensor.

4. Conclusion

An efficient DNA immobilization matrix based on polyaniline nanotube and gold nanoparticle films modified at the glassy carbon electrode was developed for the fabrication of a DNA electrochemical biosensor. This matrix incorporated the advantages of polyaniline nanotube and gold nanoparticle, which enhanced greatly the immobilization of the DNA probe on the films and the detection sensitivity of the target DNA. The DNA biosensor has been used to the detection of DNA sequence-specific of PAT gene with high sensitivity, low detection limit, wide dynamic detection range, and could effectively discriminate completely complementary target sequence, noncomplementary sequence, single-base mismatched sequence and double-base mismatched sequence.

Acknowledgements

This work was supported by the National Natural Science Foundation of China (no. 20635020, no. 20375020), Doctoral Foundation of the Ministry of Education of China (no. 20060426001) and Doctoral Fund of QUST (0022278).

REFERENCES

[1] G. Yang, W. Hou, X. Feng, L. Xu, Y. Liu, G. Wang, W. Ding, Adv. Funct. Mater. 17 (2007) 401.
[2] K. Arora, N. Prabhakar, S. Chand, B.D. Malhotra, Anal. Chem. 79 (2007) 6152.
[3] L.X. Shi, Y. Xiao, I. Willner, Electrochem. Commun. 6 (2004) 1057.
[4] Z.C. Tang, D.S. Geng, G.X. Lu, Thin Solid Films 497 (2006) 309.
[5] I. Jurevičiūtė, K. Brazdžiuvienė, L. Bernotaitė, B. Šalkus, A. Malinauskas, Sens. Actuators, B 107 (2005) 716.
[6] S. Singh, P.R. Solanki, M.K. Pandey, B.D. Malhotra, Anal. Chim. Acta 568 (2006) 126.
[7] S. Singh, P.R. Solanki, M.K. Pandey, B.D. Malhotra, Sens. Actuators, B 115 (2006) 534.
[8] A. Kumar, G. Whitaker, A. Kumar, Biosens. Bioelectron. 21 (2005) 513.
[9] J. Wu, Y.H. Zou, X.L. Li, H.B. Liu, G.L. Shen, R.Q. Yu, Sens. Actuators, B 104 (2005) 43.
[10] H.X. Chang, Y. Yuan, N.L. Shi, Y.F. Guan, Anal. Chem. 79 (2007) 5111.
[11] X.L. Luo, A.J. Killard, M.R. Smyth, Chem. Eur. J. 13 (2007) 2138.
[12] A. Morrin, O. Ngamna, A.J. Killard, S.E. Moulton, M.R. Smyth, G.G. Wallace, Electroanalysis 17 (2005) 423.
[13] H.H. Zhou, H. Chen, S.L. Luo, J.H. Chen, W.Z. Wei, Y.F. Kuang, Biosens. Bioelectron. 20 (2005) 1305.
[14] N.N. Zhu, Z. Chang, P.G. He, Y.Z. Fang, Electrochim. Acta 51 (2006) 3758.
[15] Y. Leroux, E. Eang, C. Fave, G. Trippe, J.C. Lacroix, Electrochem. Commun. 9 (2007) 1258.
[16] S. Carrara, V. Bavastrello, D. Ricci, E. Stura, C. Nicolini, Sens. Actuators, B 109 (2005) 221.
[17] E. Granot, B. Basnar, Z. Cheglakov, E. Katz, I. Willner, Electroanalysis 18 (2006) 26.
[18] Y.J. Zou, L.X. Sun, F. Xu, Biosens. Bioelectron. 22 (2007) 2669.
[19] D. Shan, S.X. Wang, Y.Y. He, H.G. Xue, Mater. Sci. Eng. 28 (2008) 213.
[20] K.M. Manesh, P. Santhosh, A.I. Gopalan, K.P. Lee, Electroanalysis 18 (2006) 1564.
[21] S.J. Tian, J.Y. Liu, T. Zhu, W. Knoll, Chem. Mater. 16 (2004) 4103.

[22] G.C. Li, S.P. Pang, G.W. Xie, Z.B. Wang, H.R. Peng, Z.K. Zhang, Polymer 47 (2006) 1456.
[23] Y.C. Tsai, S.C. Li, J.M. Chen, Langmuir 21 (2005) 3653.
[24] Y.C. Tsai, C.C. Chiu, Sens. Actuators, B 125 (2007) 10.
[25] S.F. Liu, Y.F. Li, J.R. Li, L. Jiang, Biosens. Bioelectron. 21 (2005) 789.
[26] J. Yang, T. Yang, Y.Y. Feng, K. Jiao, Anal. Biochem. 365 (2007) 24.
[27] W.R. Yang, M. Ozsoz, D.B. Hibbert, J.J. Gooding, Electroanalysis 14 (2002) 1299.
[28] J. Yang, K. Jiao, T. Yang, Anal. Bioanal. Chem. 389 (2007) 913.